Double Spherical Harmonics and The Radiative Transport Equation

Sean Horan

Overview

My goal is to explain a new, **deterministic solution** to the **Radiative Transport Equation**.

This equation governs the behavior of **radiant energy** in a **turbid medium**. Its solutions have applications in atmospheric science, reactor physics, computer graphics and **biophotonics**.

The purpose of this solution is to **accurately** and **efficiently** simulate the **behavior of light** in **layered, biological tissue**, for use in **optical imaging**.

Please **ask questions** when you have them. Your understanding of this is important to me!

Background (Or: What is he talking about and why should I care?)

Light As Particles

Light is both a **wave** and a **particle**.

We will focus on **light as a particle**.

These **particles (photons)** move through media and are **scattered** and **absorbed**.

This gives us of conception of light as **radiant energy moving through a medium**.

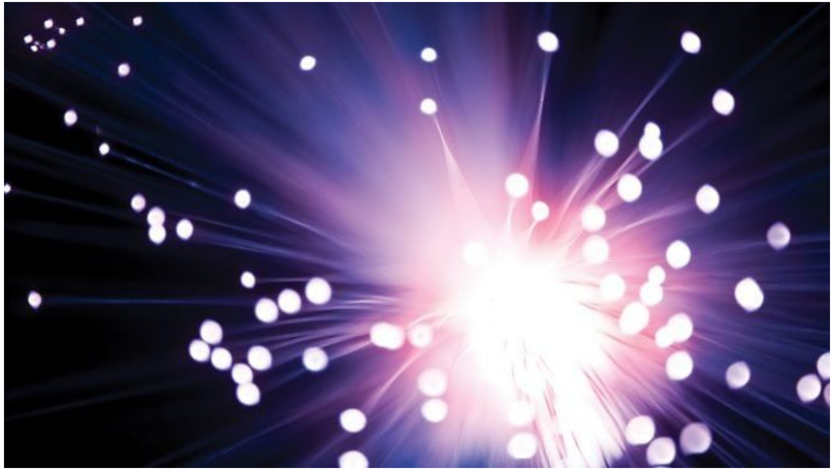

Turbid Media

Material in which **light is scattered** and **absorbed**.

The following quantities are associated with it:

- μ_s: **Scattering Coefficient**
- μ_a: **Absorption Coefficient**
- $\mu_s + \mu_a = \mu_t$: **Total Attenuation**

These have the **same units (1/mm)**. They define **length scales** over which these events occur, are are functions of **wavelength**.

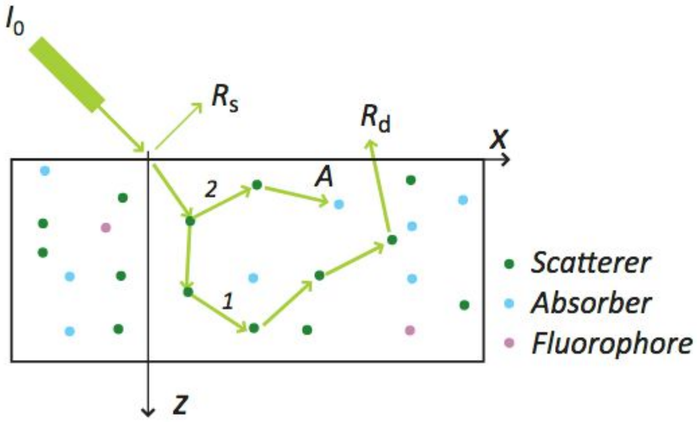

Absorption

Absorption spectra can be **highly structured**, which gives us materials of **different color**.

Particles which absorb light are known as **chromophores**.

Absorption of a medium is a **linear combination** of chromophores with weights defined by **concentration**.

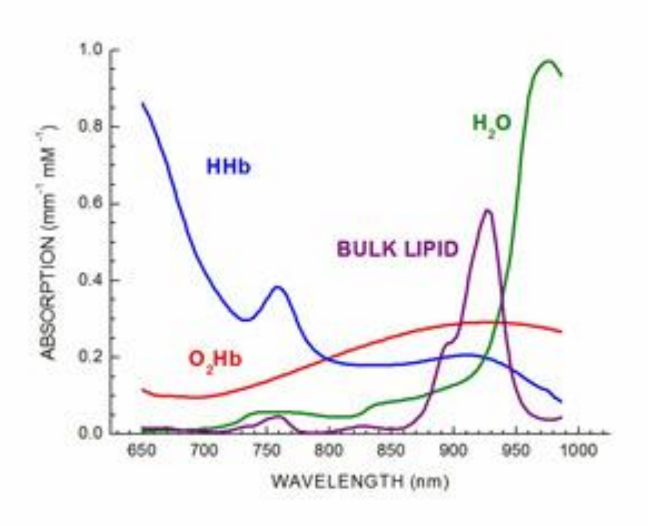

Scattering

Scattering direction is defined by the **size** and **shape** of the scattering particles.

It is described by a **scattering phase function (p)**, which defines a **probability distribution** of the **scattered direction** of a photon given its **incident direction**.

This function defines the following quantities:

- g: **Anisotropy**
- $(1-g)\mu_s = \mu_s'$: **Reduced Scattering Coefficient**
- $1/(\mu_s' + \mu_a) = l^*$: **Mean free path**

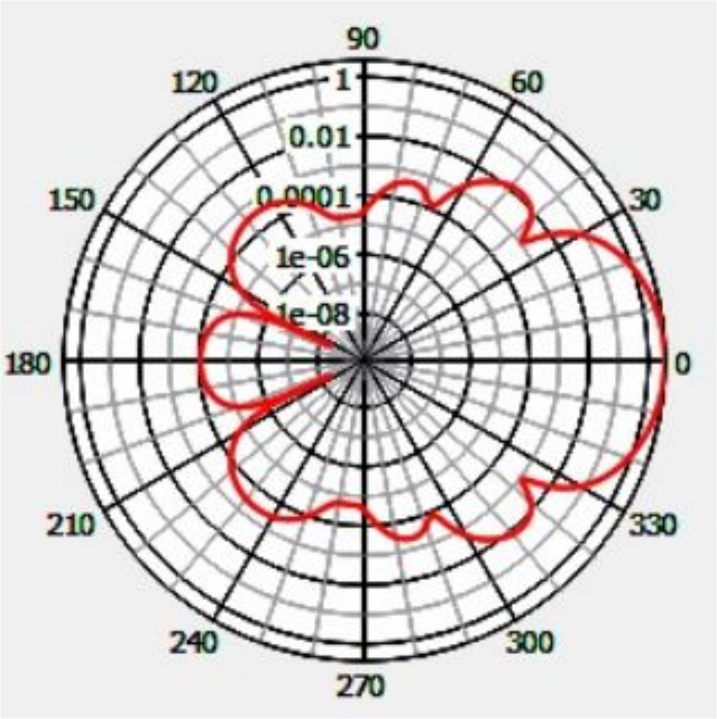

Light and Biological Tissue

How a tissue **scatters** and **absorbs** light can tell us a great deal about it.

Examples:

- Blood flow
- Tissue oxygenation
- Burn wound depth
- Breast cancer detection

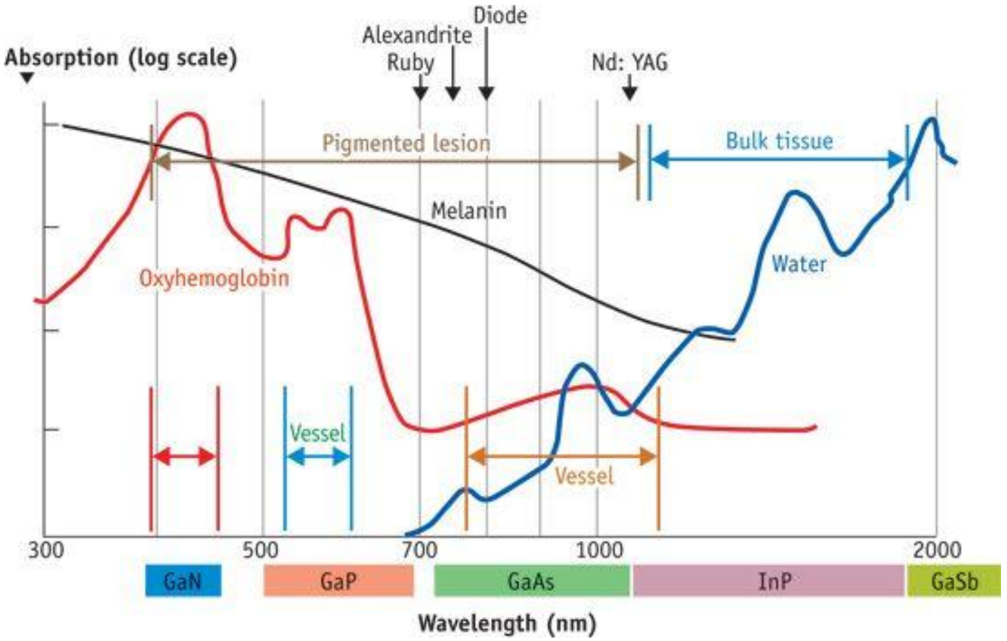

Image credit: biopticsworld.com

Optical Imaging

Physiological information can be inferred from a **tissue's optical properties**.

Common chromophores include **hemoglobin**, **oxyhemoglobin**, **bulk lipids** and **water**. [1]

Common scatterers include **cell nuclei**, **collagen fiber bundles** and some **organelles**. [2]

The **use of light** to **interrogate tissue** and obtain these, and other, **physiological properties** is called **Optical Imaging**.

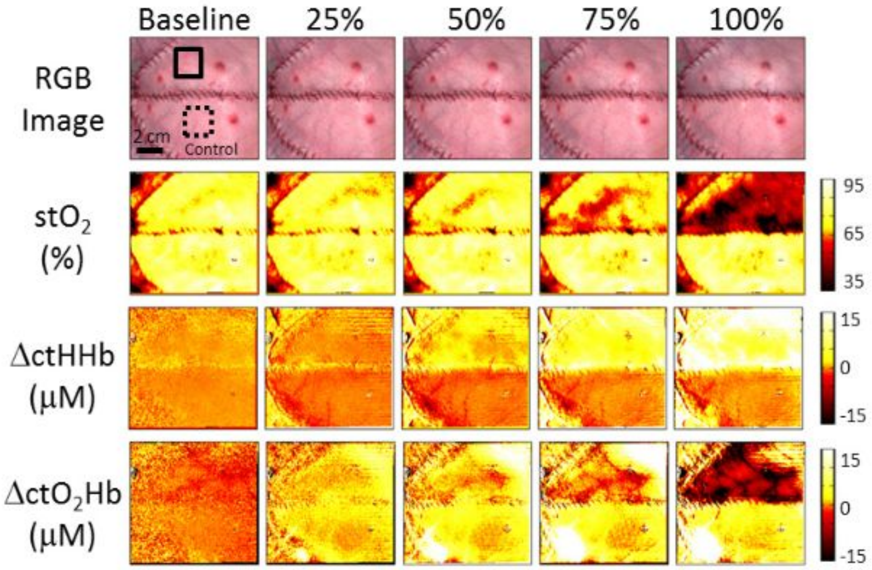

Ponticorvo, et al, Biomed Exp. 2013

Length Scales

Different conceptions of light are useful on **different length scales**.

These **length scales** define situations in which we can **model light continuously**, despite its **quantum nature**.

We will focus on length scales found in **biological tissues**.

Features at these scales (skin layer thickness, vasculature, etc) are often **larger than $1/\mu_t$**, but may be **smaller than $1/\mu_t'$**.

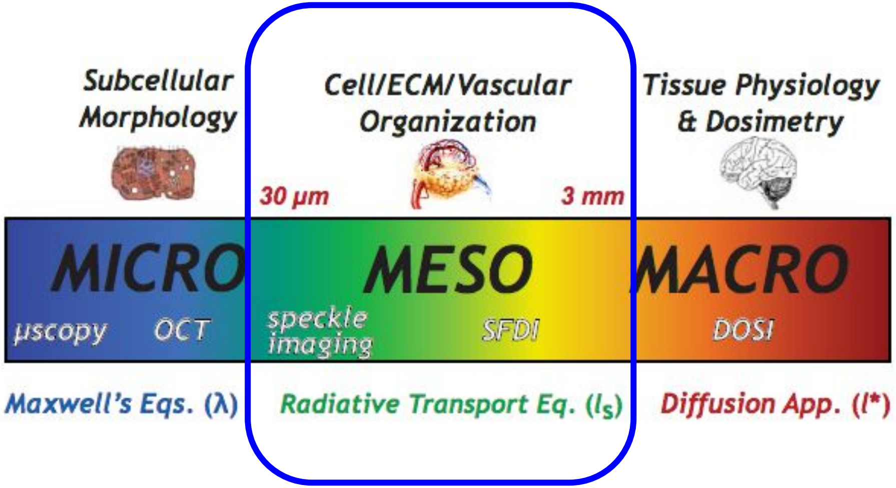

The Radiative Transport Equation

The Radiative Transport Equation (RTE)

Originally published by Eugen von Lommel in 1887, the **Radiative Transport Equation (RTE)** describes the propagation of **radiant energy** through a **scattering** and **absorbing** medium in **space** and **time**.

$$\nabla \cdot \Omega L(r, \Omega, t) + \frac{1}{c(r)} \frac{\partial}{\partial t} L(r, \Omega, t) =$$

$$-\mu_t(r) L(r, \Omega, t) + \mu_s(r) \int_{4\pi} L(r, \Omega', t) p(r, \Omega', \Omega) d\Omega' + Q(r, \Omega, t)$$

Breaking Down The RTE

The total change in **radiant energy L** at a **position r**, a **direction Ω** and a **time t** is equal to the sum of:

$$\nabla \cdot \Omega \underline{L(r,\Omega,t)} + \frac{1}{c(r)}\frac{\partial}{\partial t}\underline{L(r,\Omega,t)} =$$

Breaking Down The RTE

The total change in **radiant energy L** at a **position r**, a **direction Ω** and a **time t** is equal to the sum of:

1. Loss due to attenuation

$$\nabla \cdot \Omega \underline{L(r,\Omega,t)} + \frac{1}{c(r)}\frac{\partial}{\partial t}\underline{L(r,\Omega,t)} =$$

$$-\mu_t(r)\underline{L(r,\Omega,t)}$$

Breaking Down The RTE

The total change in **radiant energy L** at a **position r**, a **direction Ω** and a **time t** is equal to the sum of:

1. Loss due to attenuation
2. Gain due to scattering

$$\nabla \cdot \Omega \underline{L(r, \Omega, t)} + \frac{1}{c(r)} \frac{\partial}{\partial t} \underline{L(r, \Omega, t)} =$$

$$-\mu_t(r) \underline{L(r, \Omega, t)} + \mu_s(r) \int_{4\pi} \underline{L(r, \Omega', t)} p(r, \Omega', \Omega) d\Omega' .$$

Breaking Down The RTE

The total change in **radiant energy L** at a **position r**, a **direction Ω** and a **time t** is equal to the sum of:

1. Loss due to attenuation
2. Gain due to scattering
3. Gain due to sources

$$\nabla \cdot \Omega \underline{L(r,\Omega,t)} + \frac{1}{c(r)}\frac{\partial}{\partial t}\underline{L(r,\Omega,t)} =$$

$$-\mu_t(r)\underline{L(r,\Omega,t)} + \mu_s(r)\int_{4\pi}\underline{L(r,\Omega',t)}p(r,\Omega',\Omega)d\Omega' + Q(r,\Omega,t)$$

Common Simplifying Assumptions

1. **Temporal steady state (dL/dt=0)**. Most, but not all, optical imaging modalities deal with **time scales** far **greater than the time spent by photons in a medium**.

2. **Spherical scatterers**. Scattering in biological media is similar to that of **poly-dispersed spherical scatterers**. Therefore, plane waves of light can be thought of as **normally incident** on scatters. This **reduces the argument** of the **scattering phase function** at any point **r** to a **single angle**. [2]

Commonly Used Version Of The RTE

$$\nabla \cdot \Omega \underline{L(r, \Omega)} = -\mu_t(r) \underline{L(r, \Omega)} + \mu_s(r) \int_{4\pi} \underline{L(r, \Omega')} p(r, \Omega' \cdot \Omega) d\Omega' + Q(r, \Omega)$$

RTE Solutions

Stochastic Solutions (Monte Carlo)

- Analog (Howell 1968, others)
- Discrete/Continuous Absorption Weight (Spanier, Hayakawa, Venugopalan 2014) [3]

Deterministic Solutions

- **Spectral Methods**
  - Diffusion Approximation (Ishimaru, 1989) [4]
  - Green's Function (Kim, Keller, 2003, Machida et al 2013) [5,6]
  - Delta P_1 (Carp, Hayakawa, Venugopalan 2004) [7]
  - Spherical Harmonic Expansion with Fourier Coefficients ($SHEF_N$) (Gardner, 2013) [8]
- **Finite Element Method**
  - Multigrid RTE (Gao, Zhao, 2009) [9]

Solution Wish List

1. Accurately reconstruct **radiance**, as well as common **functionals of radiance**.
   a. **Fluence**
   b. **Reflectance**
   c. **Transmittance**
2. Be **robust** to wide variations in **source** and **media properties**
3. Calculate as **efficiently** as possible.
4. Be usable in **optical property recovery**

Each method has strengths and weaknesses. **No one does it all.**

Stochastic methods can be **highly accurate**, even in **complex geometries**, but are **computationally expensive**.

Deterministic methods are often much faster, but **may not be accurate** in constructing radiance at **desired length scales**.

Current Best Practice

The most accurate spectral, deterministic method for solving the RTE currently used is Adam Gardner's **Spherical Harmonic Expansion utilizing Fourier decomposition to order N ($SHEF_N$)**. [8]

This method, when combined with a **sequential order smoothing**, has shown **high levels of accuracy** in reconstructing **radiance** and **reflectance** at **medium surfaces**.

New RTE Solution Method

New Method Goals

We will **build on SHEF$_N$** by introducing a **new method** of **solving the RTE** which **does not require post-processing** for accuracy and is more **robust to parameter changes**.

This method will be capable of reconstructing **radiance** with **angular discontinuities** at **medium boundaries**, which SHEF$_N$ is not.

Assumptions

Medium is **homogeneous** and **semi-infinite**

- Infinite extent in **x and y directions**
- Infinitely deep in **z (positive) direction**
- Only **non-scattering, non-absorbing** air in **negative z direction**
- **Boundary** between air and medium is **z = 0 plane**
- **Refractive index mismatch** at boundary

Collimated source that is external to medium

  - **Decays exponentially** in **z**

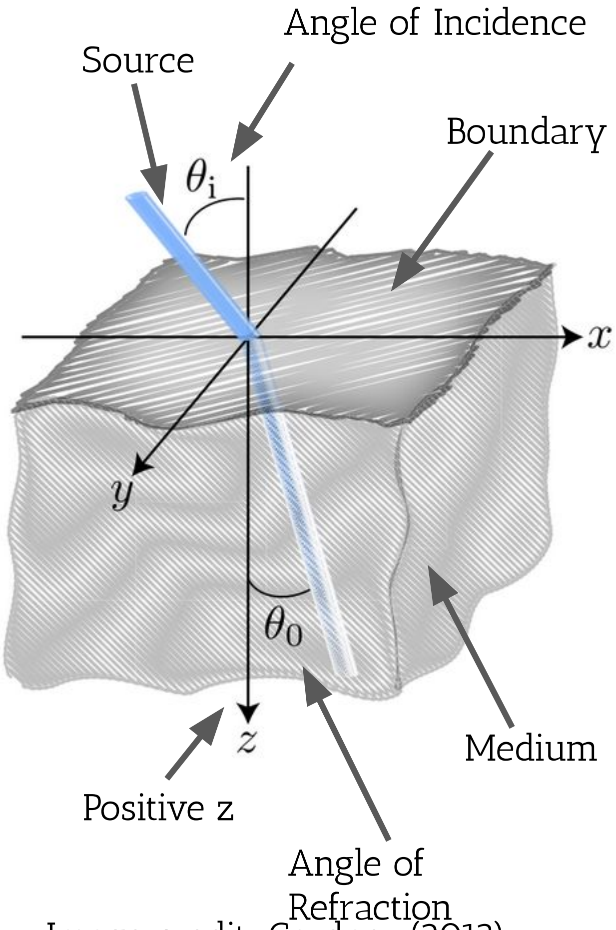

Image credit: Gardner (2013)

Double SHEF$_N$ or DSHEF Solution

Double Spherical Harmonic Expansion utilizing Fourier decomposition to order N

Deterministic, spectral method of solving the **RTE**, relying on **Fourier methods** (ideal for **spatial frequency based imaging**.)

At any point, represent **upwardly** and **downwardly** directed radiance indepently of each other, as linear combinations of compressed **Spherical Harmonic Functions**.

$$\tilde{Y}^{+}_{l,m}(\Omega) = \sqrt{2} K_{l,m} P_{l,m}\left(2\cos(\theta) - 1\right)\exp(im\phi)$$

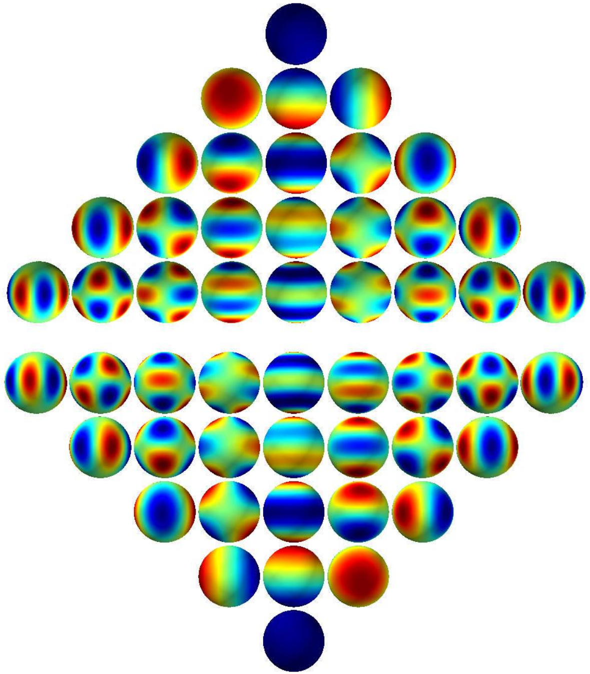

Image credit: Florian Porkony

DSHEF Solution Overview

1. Represent **scattered radiance** as a vector of **Double Spherical Harmonic Functions (DSHFs)**.
2. Convert **differential** and **integral** operators, as well **source gain** and **attenuation** terms, to matrices and vectors in a space corresponding to DSHFs.
3. Use **Fourier Transforms** in **x** and **y** to eliminate those partial derivatives to **convert the RTE into an ODE system**.
4. Calculate **particular (using source gain)** and **homogeneous (using generalized eigenvalues) solutions** by applying the **Marshak Boundary Condition**.

Scattered Radiance

Scattered Radiance (Ψ) is represented as a **linear combination** of **DSHFs**, with moments considered to be **smooth functions of position**.

$$\underline{\Psi(r,\Omega)} = \sum_{l,m}\left[\chi_{\theta\le\frac{\pi}{2}}\underline{\psi^{+}_{l,m}}(r)\,\tilde{Y}^{+}_{l,m}(\Omega) + \chi_{\theta>\frac{\pi}{2}}\underline{\psi^{-}_{l,m}}(r)\,\tilde{Y}^{-}_{l,m}(\Omega)\right]$$

Therefore, at any point in space, the angular distribution of radiance is represented as **a single point in R^M**, where $M=2(N+1)^2$. Thus, we think of **Ψ as a point in R^M**.

$$\underline{\Psi} = \begin{bmatrix} \underline{\Psi^{+}} \\ \underline{\Psi^{-}} \end{bmatrix}$$

The $DSHEF_N$ method relies on solving the RTE in this context, ultimately constructing a **smooth function from R to R^M**.

Differential Term

Expanding the **directional derivative** in **Cartesian coordinates** and taking **L^2 inner products** gives recurrence relations:

$$A_x^+(l, m \to l', m') = \left\langle \tilde{Y}_{l,m}^+, \sin(\theta)\cos(\phi)\tilde{Y}_{l',m'}^+ \right\rangle$$

$$\Big[\sum A_x^+(l \pm 1, m \pm 1 \to l, m)\frac{\partial}{\partial x}\psi^+_{\underline{l\pm1,m\pm1}}(r) +$$

$$\sum A_y^+(l \pm 1, m \pm 1 \to l, m)\frac{\partial}{\partial y}\psi^+_{\underline{l\pm1,m\pm1}}(r) +$$

$$\sum A_z^+(l \pm 1, m \to l, m)\frac{\partial}{\partial z}\psi^+_{\underline{l\pm1,m}}(r)\Big]\tilde{Y}_{l,m}^+(\Omega)$$

Differential Term

This leads to the construction of **three matrices** based on **recurrence relations**:

$$\nabla \cdot \Omega \underline{\Psi} = \begin{bmatrix} A_x & 0 \\ 0 & A_x \end{bmatrix} \frac{\partial \Psi}{\underline{\partial x}} + \begin{bmatrix} A_y & 0 \\ 0 & A_y \end{bmatrix} \frac{\partial \Psi}{\underline{\partial y}} + \begin{bmatrix} A_z & 0 \\ 0 & -A_z \end{bmatrix} \frac{\partial \Psi}{\underline{\partial z}}$$

Integral Term

The **integral operator** is converted by first expanding the **scattering phase function** in terms of **single spherical harmonics**, then converting to **double spherical harmonics** by a **conversion matrix C**.

This is done to **preserve cross talk** between **upwardly** and **downwardly** directed **scattered radiance**.

$$\mu_s \int_{4\pi} \Psi\left(r, \Omega'\right) p(\Omega' \cdot \Omega) d\Omega'$$

$$p\left(\Omega' \cdot \Omega\right) = \sum_l (2l+1) g_l \sum_{m=-l}^{l} 4\pi Y_{l,m}^{*}(\Omega') Y_{l,m}(\Omega)$$

$$Y_{l,m} = \sum_{l'} c^{\pm}(l, m \to l', m) \tilde{Y}_{l',m}^{\pm}$$

$$p\left(\Omega' \cdot \Omega\right) = \sum_l g_l \sum_{m=-l}^{l} 4\pi \left[\sum_{l'} c^{\pm}(l, m \to l', m) \tilde{Y}_{l',m}^{\pm,*}(\Omega')\right] \left[\sum_{l'} c^{\pm}(l, m \to l', m) \tilde{Y}_{l',m}^{\pm}(\Omega)\right]$$

Integral Term

We then integrate to reduce this term exploiting **orthonormality** to another series of **recurrence relations**:

$$\int_{4\pi} \bar{Y}^{+}_{l,m}(\Omega')\underline{p(\Omega' \cdot \Omega)}d\Omega' = \sum_{l'} \underline{g_{l'}} 4\pi \left[\sum_{l'} c^{\pm}(l', m \to l, m)\,(\pm\delta_{l,l'})\right] \left[\sum_{l'} c^{+}(l', m \to l, m)\right] \tilde{Y}^{+}_{l,m}(\Omega)$$

As with the **differential operator**, these terms create a **block matrix**. Unlike the **differential operator**, the **off diagonal blocks are nonzero**:

$$\mu_s \int_{4\pi} \underline{\Psi\left(r, \Omega'\right)}\, \underline{p(\Omega' \cdot \Omega)}d\Omega' = \underline{\begin{bmatrix} P_1 & P_2 \\ P_2 & P_1 \end{bmatrix}}\, \underline{\Psi}$$

P_1 governs scattering **within one hemisphere**. **P_2** governs scattering from **one hemisphere to another**. It is important to note that they act **without an absolute frame of reference**.

Source Term

The source term is the **contribution to scattered radiance** from our **collimated source**.

It **decays exponentially** in **z** at a rate of μ_t/μ_0 and at **z=0** has moments given by the **scattering phase function**.

Expansion in the **same manner as the scattering phase function** yields:

$$Q(z) = 4\pi\mu_s C \exp\left(\frac{\mu_t}{\mu_0} z\right) \sum_{l'} g_{l'} 4\pi \left[\sum_{l'} c^{\pm}(l', m \to l, m)\,(\pm\delta_{l,l'})\right] \left[\sum_{l'} c^{\pm}(l', m \to l, m)\right] \tilde{Y}^{\pm}_{l,m}(\Omega)$$

IDE to PDEs to ODEs

We have now **converted the RTE** from an **integral-differential equation** to a **system of partial differential equations**:

$$A_x \frac{\partial}{\partial x}\underline{\Psi}(r) + A_y \frac{\partial}{\partial y}\underline{\Psi}(r) + A_z \frac{\partial}{\partial z}\underline{\Psi}(r) = -\mu_t \underline{\Psi}(r) + P\underline{\Psi}(r) + Q(r)$$

This can then be converted to a **system of ordinary differential equations** by means of **Fourier Transforms in x and y**:

$$A_z \frac{d}{dz}\underline{\tilde{\Psi}}(z, k_x, k_y) = -2\pi k_x A_x \underline{\tilde{\Psi}}(z, k_x, k_y) - 2\pi k_y A_y \underline{\tilde{\Psi}}(z, k_x, k_y)$$
$$- \mu_t \underline{\tilde{\Psi}}(z, k_x, k_y) + P\underline{\tilde{\Psi}}(z, k_x, k_y) + \tilde{Q}(z, k_x, k_y)$$

ODE System In Matrix Form

We can then complete our conversion of the original equation into **matrix form**, based upon the recurrence relations created and fixed wave numbers:

$$\nabla \cdot \Omega\Psi(r,\Omega) = -\mu_t \Psi(r,\Omega) + \mu_s \int_{4\pi} \Psi(r,\Omega') p(\Omega' \cdot \Omega)\, d\Omega' + Q(r,\Omega)$$

$$\Downarrow$$

$$\underbrace{\begin{bmatrix} A_z & 0 \\ 0 & -A_z \end{bmatrix}}_{A} \frac{d}{dz} \begin{bmatrix} \tilde{\Psi}^+ \\ \tilde{\Psi}^- \end{bmatrix} + \underbrace{\begin{bmatrix} -\mu_s P^+ + \mu_t I - k_x A_x - k_y A_y & -\mu_s P^- \\ -\mu_s P^- & -\mu_s P^+ + \mu_t I - k_x A_x - k_y A_y \end{bmatrix}}_{B} \begin{bmatrix} \tilde{\Psi}^+ \\ \tilde{\Psi}^- \end{bmatrix} = \begin{bmatrix} \tilde{Q}^+ \\ \tilde{Q}^- \end{bmatrix}$$

$$A\tilde{\Psi}'(z) + B\tilde{\Psi}(z) = \tilde{Q}(z)$$

Particular Solution

Our solution has **two components**: **particular** and **homogeneous**. The particular is the more straightforward to obtain with an ansatz assuming the **same decay** as the **source gain term**:

$$\underline{\tilde{\Psi}} = \underline{\tilde{\Psi}}^{(p)} + \underline{\tilde{\Psi}}^{(h)}$$

$$A\underline{\tilde{\Psi}}'(z) + B\underline{\tilde{\Psi}}(z) = \tilde{Q}(z)$$

$$\underline{\tilde{\Psi}}^{p}(z) = \left(-\frac{\mu_t}{\mu_0}A + B\right)^{-1}\tilde{Q}(z)$$

Homogeneous Solution

The homogeneous solution is more difficult, and may be defined an ansatz leading to the **generalized eigenvalue problem**:

$$A\underline{\tilde{\Psi}'}(z) = -B\underline{\tilde{\Psi}}(z)$$

$$\underline{\tilde{\Psi}}^h = \sum_i \underline{w_i} G_i \exp\left(\frac{z}{\lambda_i}\right)$$

$$AG_i = -\lambda_i BG_i$$

From here, we see that **solving the problem is equivalent to calculating w_i**.

It is important to note that **only negative lambda** terms will be included in the solution.

Boundary Conditions

Now, we use the **Marshak Boundary Condition**, which states that **downwardly directed scattered radiance** at the **boundary** must have been **upwardly directed radiance** which was **internally reflected**:

$$\int_{\theta<\frac{\pi}{2}} \underline{\Psi(z} = 0, \Omega)\tilde{Y}^{+;*}_{\Lambda,M}(\Omega)d\Omega = \int_{\theta>\frac{\pi}{2}} \underline{\Psi(z} = 0, \Omega)\gamma_F(-\cos(\theta))\tilde{Y}^{-;*}_{\Lambda,M}(\Omega)d\Omega$$

This simplifies to a matrix in whose **null space** the RTE solution **must belong**:

$$\begin{bmatrix} I & -R \end{bmatrix} \underline{\tilde{\Psi}(0)} = J\tilde{\Psi}(0) = 0$$

$$J\underline{\tilde{\Psi}^h}(0) = -J\tilde{\Psi}^p(0)$$

$$JG\underline{w} = -J\tilde{\Psi}^p(0)$$

A simple matrix inversion will calculate **w** and thus **complete the solution**.

Multi Layer DSHEF

Layered Medium Structure

Medium now composed of **multiple heterogeneous layers**.

- Different **absorption**, **scattering coefficients** and **phase functions** in each layer
- Mimics structure of **biological tissue**
- **No refractive index mismatch** between layers

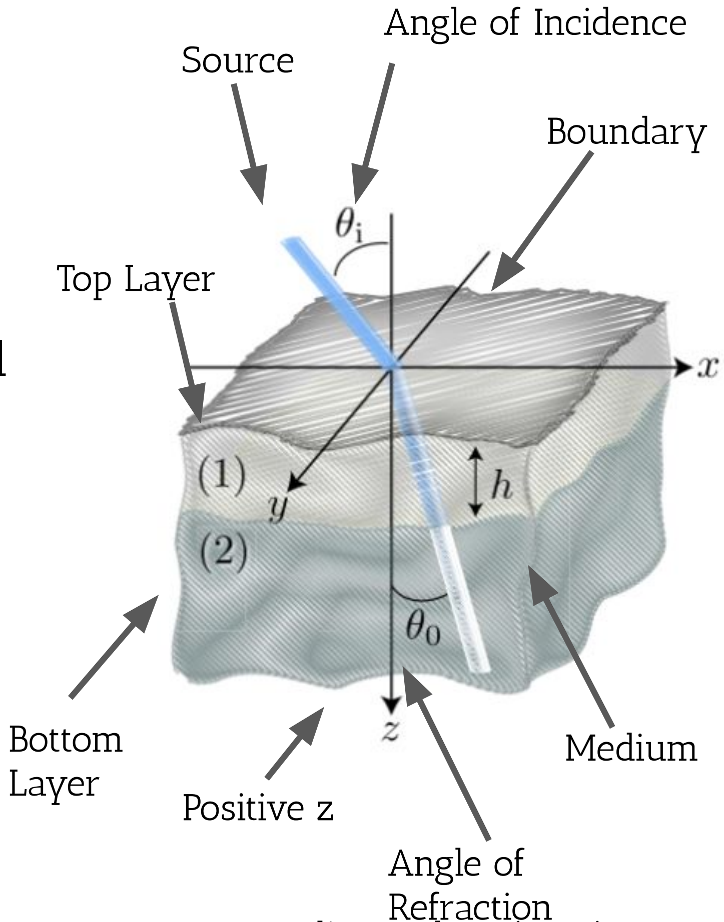

Image credit: Gardner (2012)

Solution Method For K Layers

Multilayer DSHEF relies on computing the solution to each layer as a **coupled system**. The coupling occurs by **matching radiance at layer boundaries (z_i^*)**:

$$\nabla \cdot \Omega \underline{L_i}(r,\Omega) = -\mu_{t,i}\underline{L_i}(r,\Omega) + \mu_{s,i}\int_{4\pi}\underline{L_i}(r,\Omega')p_i(\Omega'\cdot\Omega)d\Omega' + Q_i(r,\Omega)$$

$$\begin{aligned}
A_1\underline{\tilde{\Psi}'_1} + B_1\underline{\tilde{\Psi}_1} &= \tilde{Q}_1 \qquad & \underline{\tilde{\Psi}_1}\left(z=z_1^*\right) &= \underline{\tilde{\Psi}_2}\left(z=z_1^*\right)\\
A_2\underline{\tilde{\Psi}'_2} + B_2\underline{\tilde{\Psi}_2} &= \tilde{Q}_2 \qquad & \underline{\tilde{\Psi}_2}\left(z=z_2^*\right) &= \underline{\tilde{\Psi}_3}\left(z=z_2^*\right)\\
&\cdots & &\cdots\\
A_K\underline{\tilde{\Psi}'_K} + B_K\underline{\tilde{\Psi}_K} &= \tilde{Q}_K \qquad & \underline{\tilde{\Psi}_{K-1}}\left(z=z_{K-1}^*\right) &= \underline{\tilde{\Psi}_K}\left(z=z_{K-1}^*\right)
\end{aligned}$$

Eigenpair Structure in Layered System

Finite layer thickness means that **eigenpairs with positive and negative values** will now be used in the **layers 1 through K-1**. Only **negative eigenpairs** will be used in **layer K**.

We will denote **positive** and **negative** eigenvector matrices in **layer i** as $\mathbf{G_i^+}$ and $\mathbf{G_i^-}$, respectively.

We will also denote **weight vectors** in **layer i** corresponding to **positive** and **negative** eigenvectors as $\mathbf{w_i^+}$ and $\mathbf{w_i^-}$, respectively.

Weights for **positive eigenvectors** in **layer i** will be calculated using $\mathbf{z=z_i^*}$.

Weights for **negative eigenvectors** in **layer i** will be calculated using $\mathbf{z=z_{i-1}^*}$.

Boundary Conditions Between Layers

Radiance equality at **layer boundaries** creates the following:

$$\underline{\tilde{\Psi}^{h}_{i+1}}\left(z = z_i^*\right) - \underline{\tilde{\Psi}^{h}_{i}}\left(z = z_i^*\right) = \tilde{\Psi}^{p}_{i}\left(z = z_i^*\right) - \tilde{\Psi}^{p}_{i+1}\left(z = z_i^*\right) := \Delta_{i,i+1}$$

$$G^{+}_{i+1}\underline{w^{+}_{i+1}} + G^{-}_{i+1}\underline{w^{-}_{i+1}} \exp\left(\frac{z^*_{i+1} - z^*_i}{\lambda^{+}_{i+1}}\right) - G^{+}_{i+1}\underline{w^{+}_{i+1}} \exp\left(\frac{z^*_{i-1} - z^*_i}{\lambda^{+}_{i}}\right) - G^{-}_{i+1}\underline{w^{-}_{i+1}} = \Delta_{i,i+1}$$

Boundary Conditions

Boundary conditions between layers and at **z=0** are **applied concurrently** in a **single matrix inversion** to calculate **all weight vectors** (3 layer example shown):

$$\begin{bmatrix} JG^{1,+} & JG^{1,-}\exp\left(\frac{z_1^*}{\lambda_1^-}\right) & 0 & 0 & 0 \\ -G^{1,+}\exp\left(\frac{z_1^*}{\lambda_1^+}\right) & -G^{1,-} & G^{2,+} & G^{2,-}\exp\left(\frac{(z_2^*-z_3^*)}{\lambda_2^+}\right) & 0 \\ 0 & 0 & -G^{2,+}\exp\left(\frac{(z_3^*-z_2^*)}{\lambda_2^+}\right) & -G^{2,-} & G^{3,+} \end{bmatrix} \begin{bmatrix} w_1^+ \\ w_1^- \\ w_2^+ \\ w_2^- \\ w_3^+ \end{bmatrix} = \begin{bmatrix} J\tilde{\Psi}_1^{(p)}(0) \\ \Delta_{1,2} \\ \Delta_{2,3} \end{bmatrix}$$

Results

We will consider results for a **2 layered medium**.

Each layer will have a refractive index **n=1.4** and **l^*=1mm** with a **Henyey-Greenstein** scattering phase function, **anisotropy g=0.8**.

Top layer:

- **Thickness 0.1mm or 1mm**
- $\mu_s'/\mu_a = 3$

Bottom layer:

- **Semi-infinite**
- $\mu_s'/\mu_a = 100$

Results will be shown for **multiple spatial frequencies** and **orders of expansion**.

Comparison to **single SHEF$_{13}$** and a **Monte Carlo "gold standard"** will also be shown.

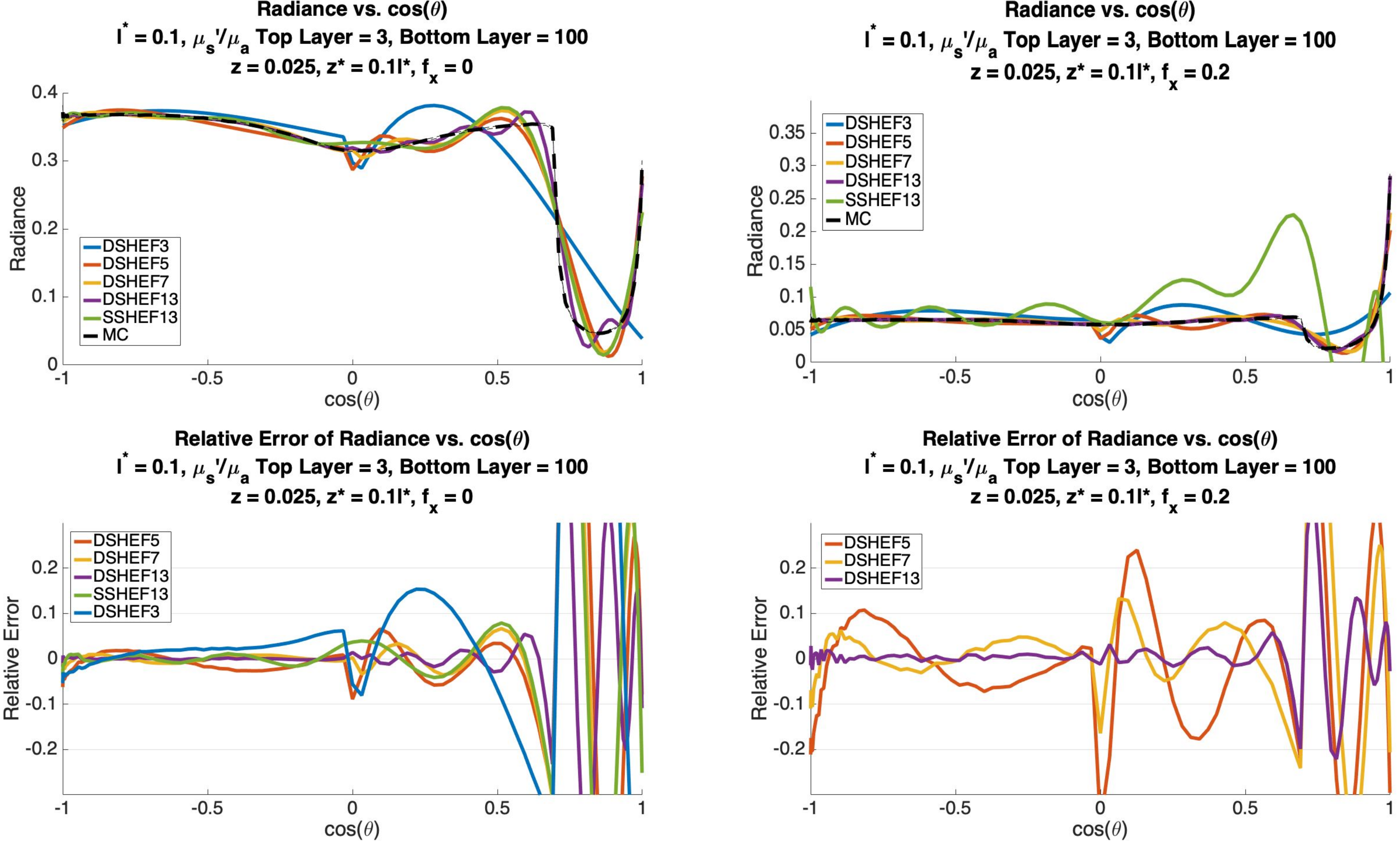

Radiance vs. cos(θ)
l* = 0.1, μs'/μa Top Layer = 3, Bottom Layer = 100
z = 0.025, z* = 0.1l*, fx = 0
Radiance
cos(θ)
DSHEF3
DSHEF5
DSHEF7
DSHEF13
SSHEF13
MC
Radiance vs. cos(θ)
l* = 0.1, μs'/μa Top Layer = 3, Bottom Layer = 100
z = 0.025, z* = 0.1l*, fx = 0.2
Radiance
cos(θ)
DSHEF3
DSHEF5
DSHEF7
DSHEF13
SSHEF13
MC
Relative Error of Radiance vs. cos(θ)
l* = 0.1, μs'/μa Top Layer = 3, Bottom Layer = 100
z = 0.025, z* = 0.1l*, fx = 0
Relative Error
cos(θ)
DSHEF5
DSHEF7
DSHEF13
SSHEF13
DSHEF3
Relative Error of Radiance vs. cos(θ)
l* = 0.1, μs'/μa Top Layer = 3, Bottom Layer = 100
z = 0.025, z* = 0.1l*, fx = 0.2
Relative Error
cos(θ)
DSHEF5
DSHEF7
DSHEF13

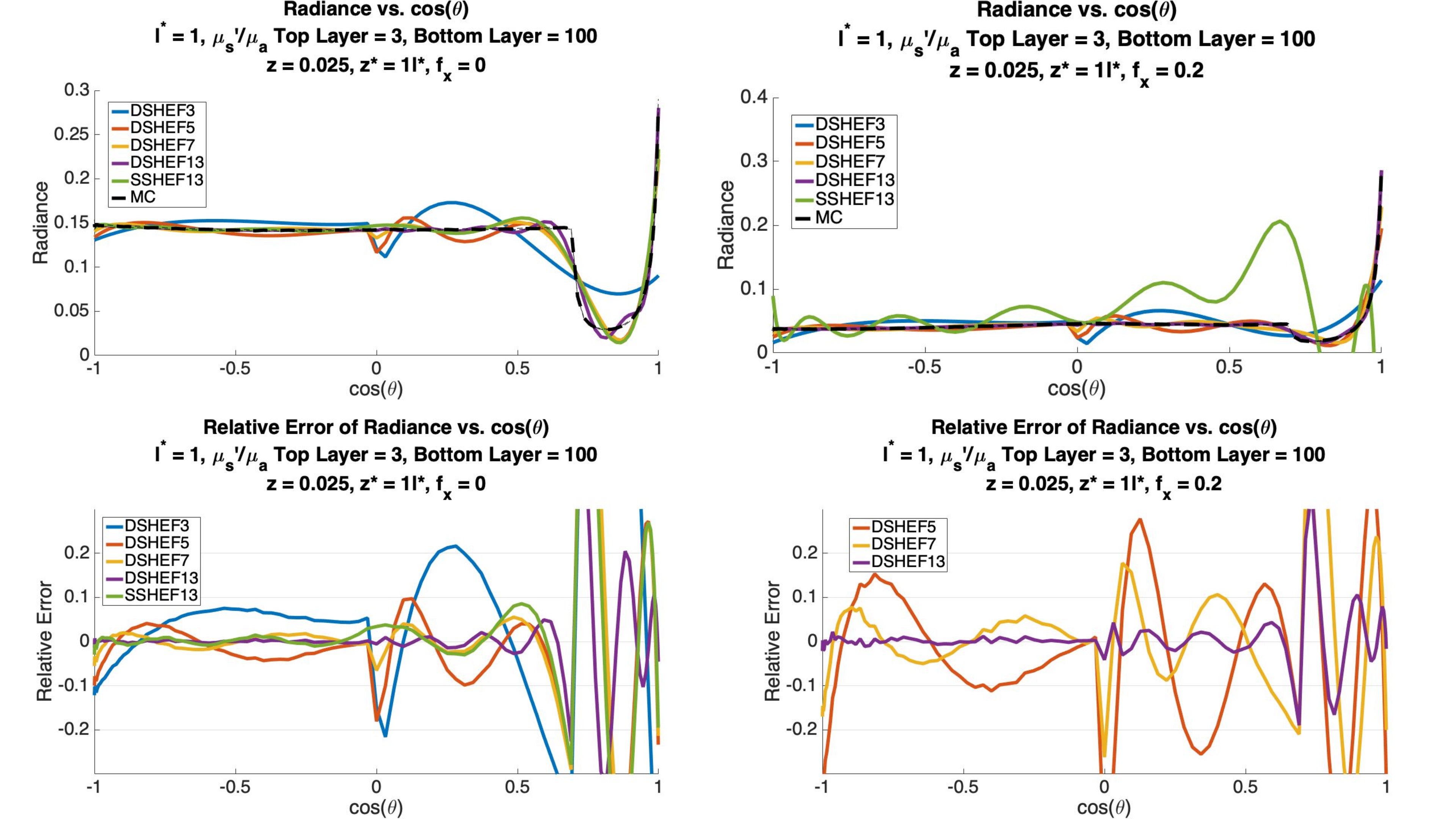
Radiance vs. cos(θ)
l* = 1, μs'/μa Top Layer = 3, Bottom Layer = 100
z = 0.025, z* = 1l*, fx = 0
DSHEF3
DSHEF5
DSHEF7
DSHEF13
SSHEF13
MC
Radiance
cos(θ)
Radiance vs. cos(θ)
l* = 1, μs'/μa Top Layer = 3, Bottom Layer = 100
z = 0.025, z* = 1l*, fx = 0.2
DSHEF3
DSHEF5
DSHEF7
DSHEF13
SSHEF13
MC
Radiance
cos(θ)
Relative Error of Radiance vs. cos(θ)
l* = 1, μs'/μa Top Layer = 3, Bottom Layer = 100
z = 0.025, z* = 1l*, fx = 0
DSHEF3
DSHEF5
DSHEF7
DSHEF13
SSHEF13
Relative Error
cos(θ)
Relative Error of Radiance vs. cos(θ)
l* = 1, μs'/μa Top Layer = 3, Bottom Layer = 100
z = 0.025, z* = 1l*, fx = 0.2
DSHEF5
DSHEF7
DSHEF13
Relative Error
cos(θ)

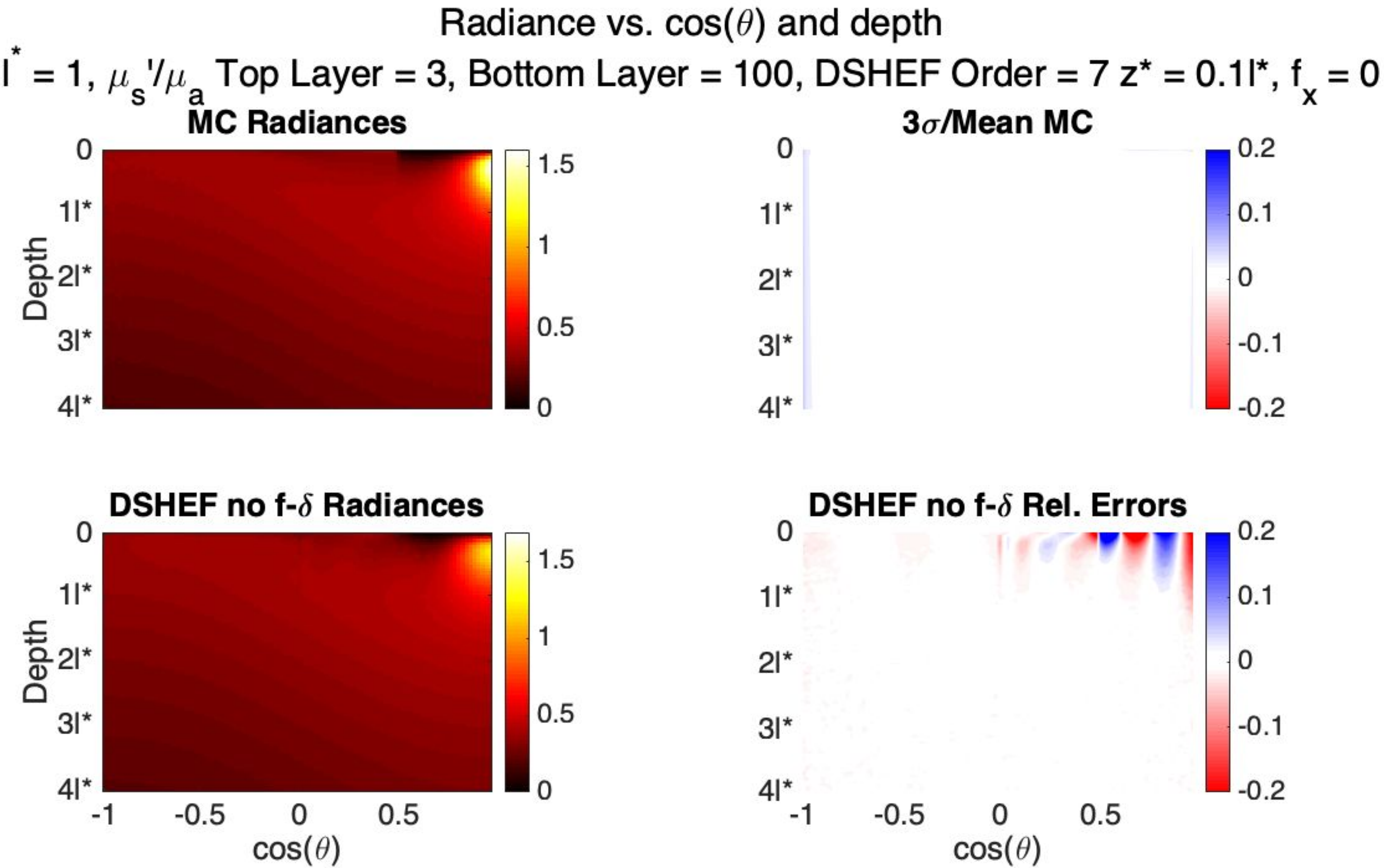
Radiance vs. cos(θ) and depth
l* = 1, μs'/μa Top Layer = 3, Bottom Layer = 100, DSHEF Order = 7 z* = 0.1l*, fx = 0
MC Radiances
3σ/Mean MC
DSHEF no f-δ Radiances
DSHEF no f-δ Rel. Errors
Depth
0
1l*
2l*
3l*
4l*
cos(θ)
-1
-0.5
0
0.5
1.5
1
0.2
0.1
-0.1
-0.2

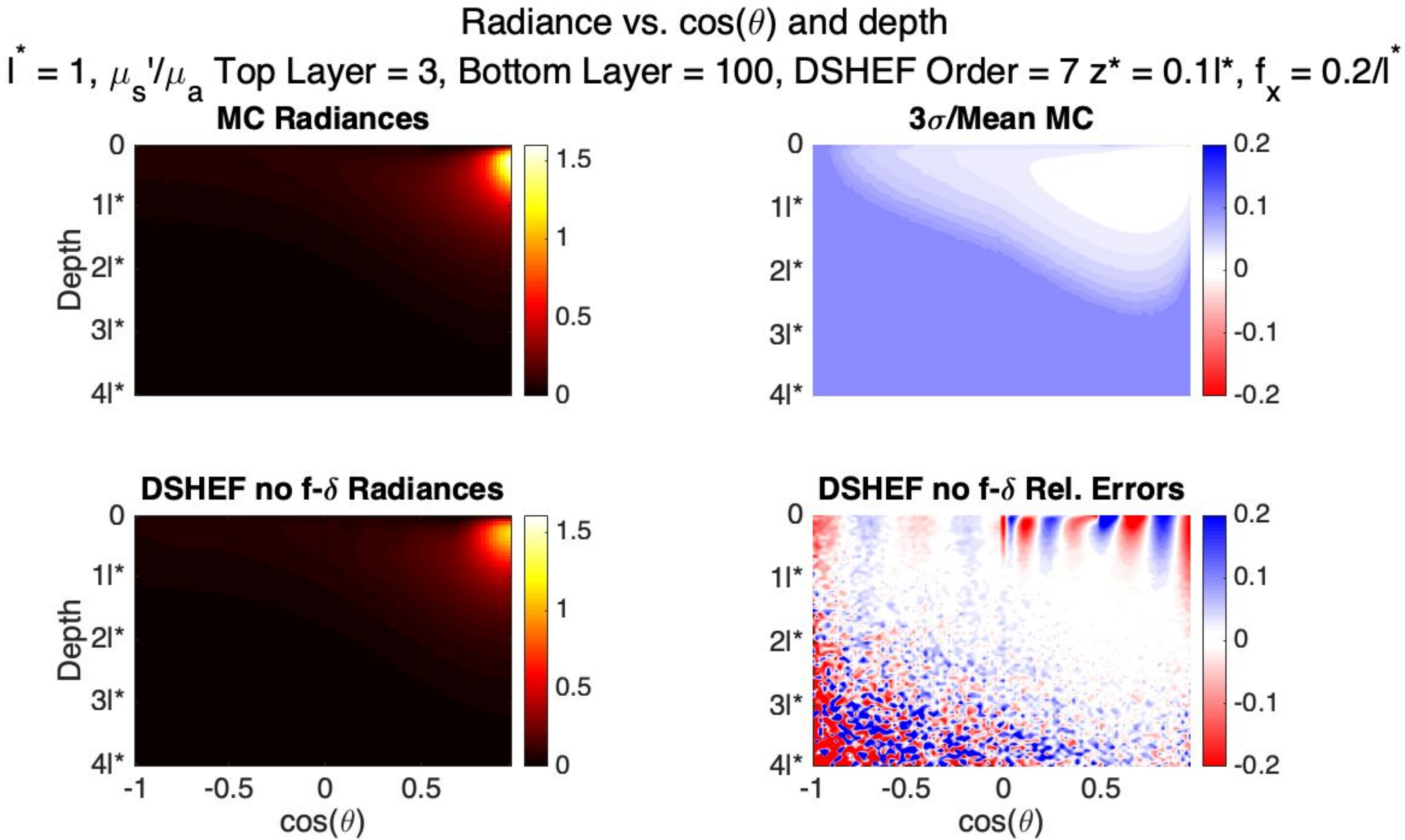
Radiance vs. cos(θ) and depth
$l^* = 1$, μ_s'/μ_a Top Layer = 3, Bottom Layer = 100, DSHEF Order = 7 $z^* = 0.1l^*$, $f_x = 0.2/l^*$
MC Radiances
3σ/Mean MC
DSHEF no f-δ Radiances
DSHEF no f-δ Rel. Errors
Depth
0
1l*
2l*
3l*
4l*
0
0.5
1
1.5
-0.2
-0.1
0
0.1
0.2
-1
-0.5
0
0.5
cos(θ)

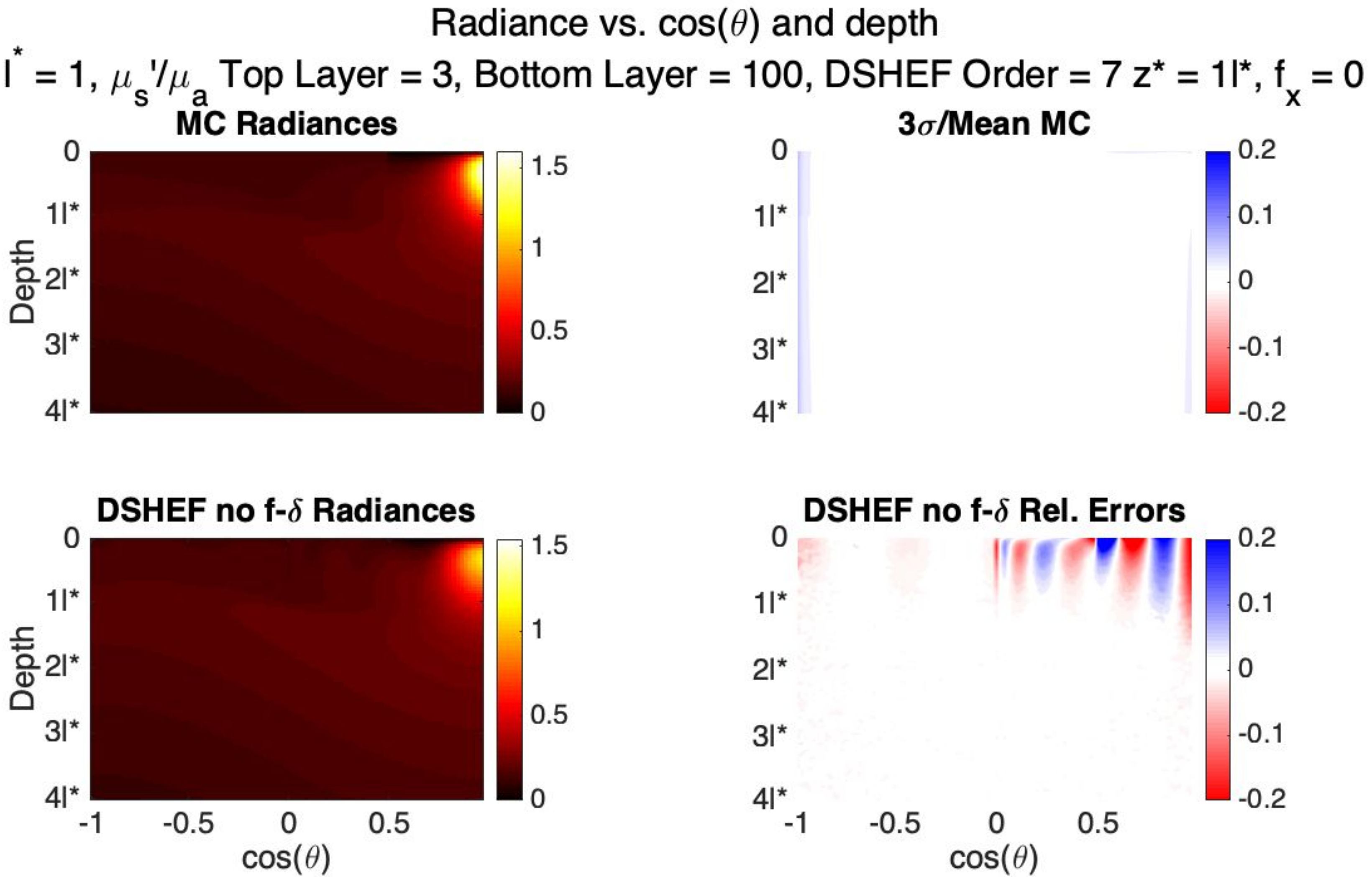

Radiance vs. cos(θ) and depth
$l^* = 1$, μ_s'/μ_a Top Layer = 3, Bottom Layer = 100, DSHEF Order = 7 $z^* = 1l^*$, $f_x = 0$
MC Radiances
3σ/Mean MC
DSHEF no f-δ Radiances
DSHEF no f-δ Rel. Errors
Depth
cos(θ)
0
1l*
2l*
3l*
4l*
-1
-0.5
0
0.5
1.5
1
0.5
0
0.2
0.1
0
-0.1
-0.2

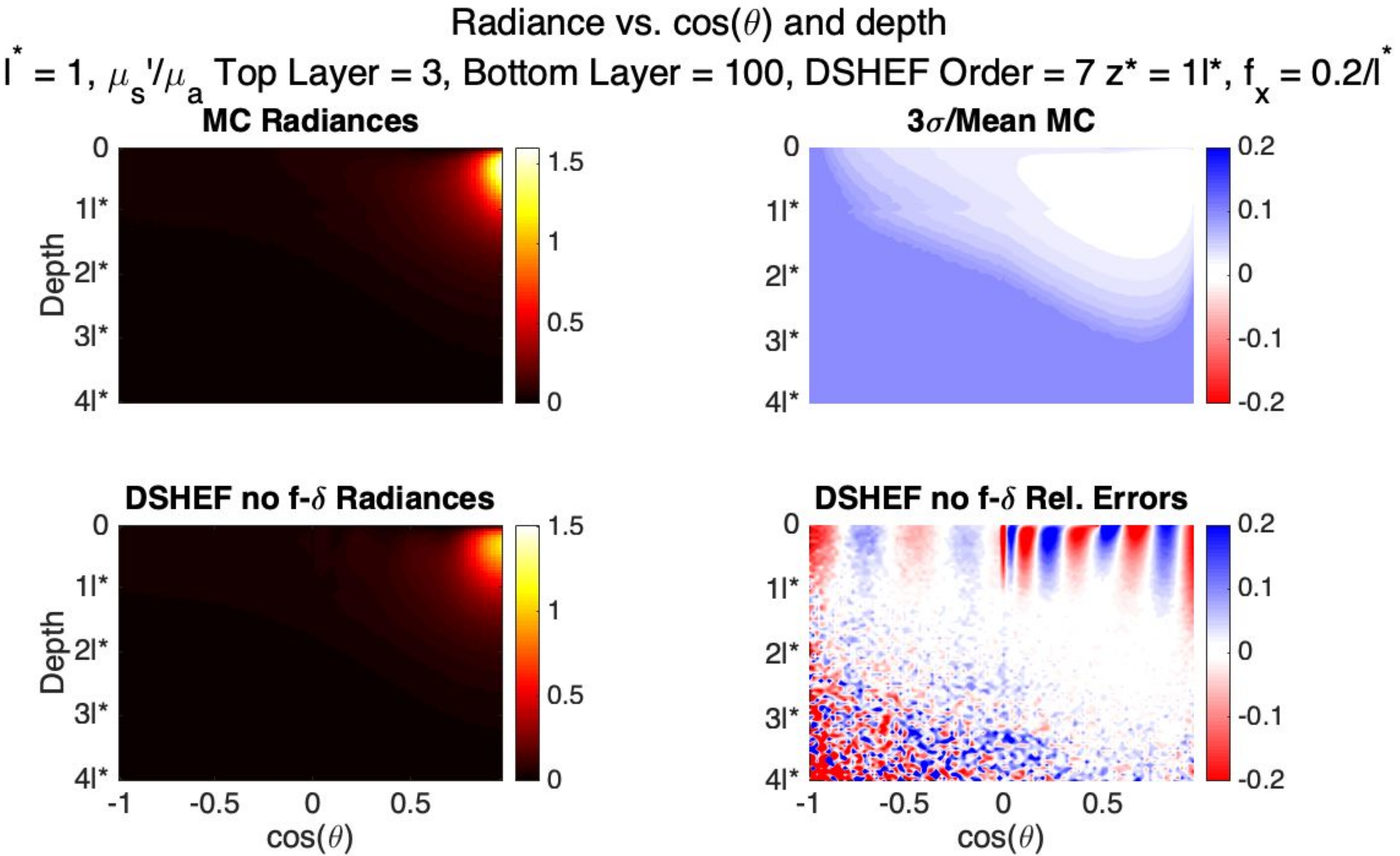

Radiance vs. cos(θ) and depth
l* = 1, μs'/μa Top Layer = 3, Bottom Layer = 100, DSHEF Order = 7 z* = 1l*, fx = 0.2/l*
MC Radiances
3σ/Mean MC
DSHEF no f-δ Radiances
DSHEF no f-δ Rel. Errors
Depth
cos(θ)
0
1l*
2l*
3l*
4l*
-1
-0.5
0
0.5
1.5
1
0.5
0
0.2
0.1
0
-0.1
-0.2

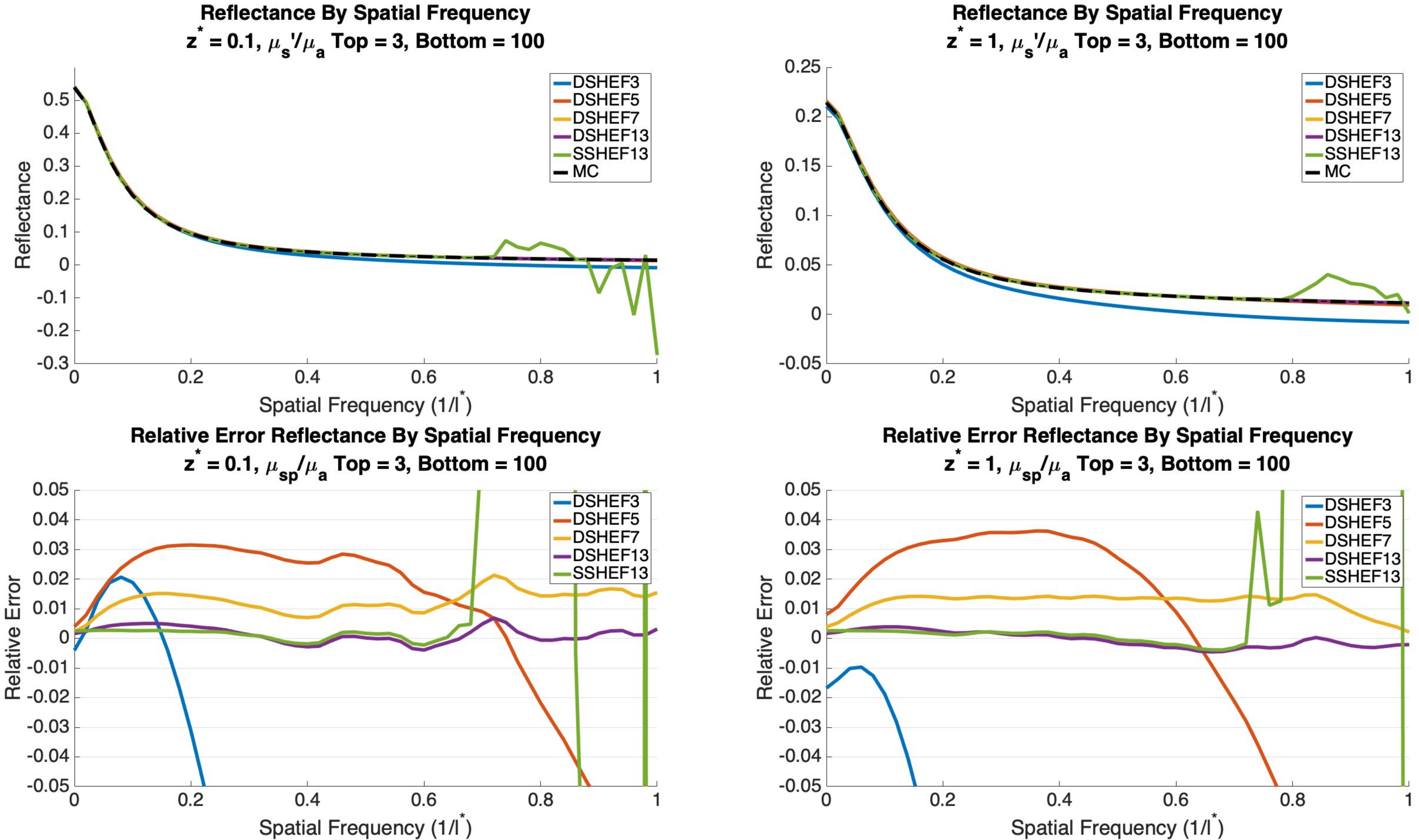
Reflectance By Spatial Frequency
z* = 0.1, μs'/μa Top = 3, Bottom = 100
Reflectance
Spatial Frequency (1/l*)
DSHEF3
DSHEF5
DSHEF7
DSHEF13
SSHEF13
MC
Reflectance By Spatial Frequency
z* = 1, μs'/μa Top = 3, Bottom = 100
Reflectance
Spatial Frequency (1/l*)
DSHEF3
DSHEF5
DSHEF7
DSHEF13
SSHEF13
MC
Relative Error Reflectance By Spatial Frequency
z* = 0.1, μsp/μa Top = 3, Bottom = 100
Relative Error
Spatial Frequency (1/l*)
DSHEF3
DSHEF5
DSHEF7
DSHEF13
SSHEF13
Relative Error Reflectance By Spatial Frequency
z* = 1, μsp/μa Top = 3, Bottom = 100
Relative Error
Spatial Frequency (1/l*)
DSHEF3
DSHEF5
DSHEF7
DSHEF13
SSHEF13

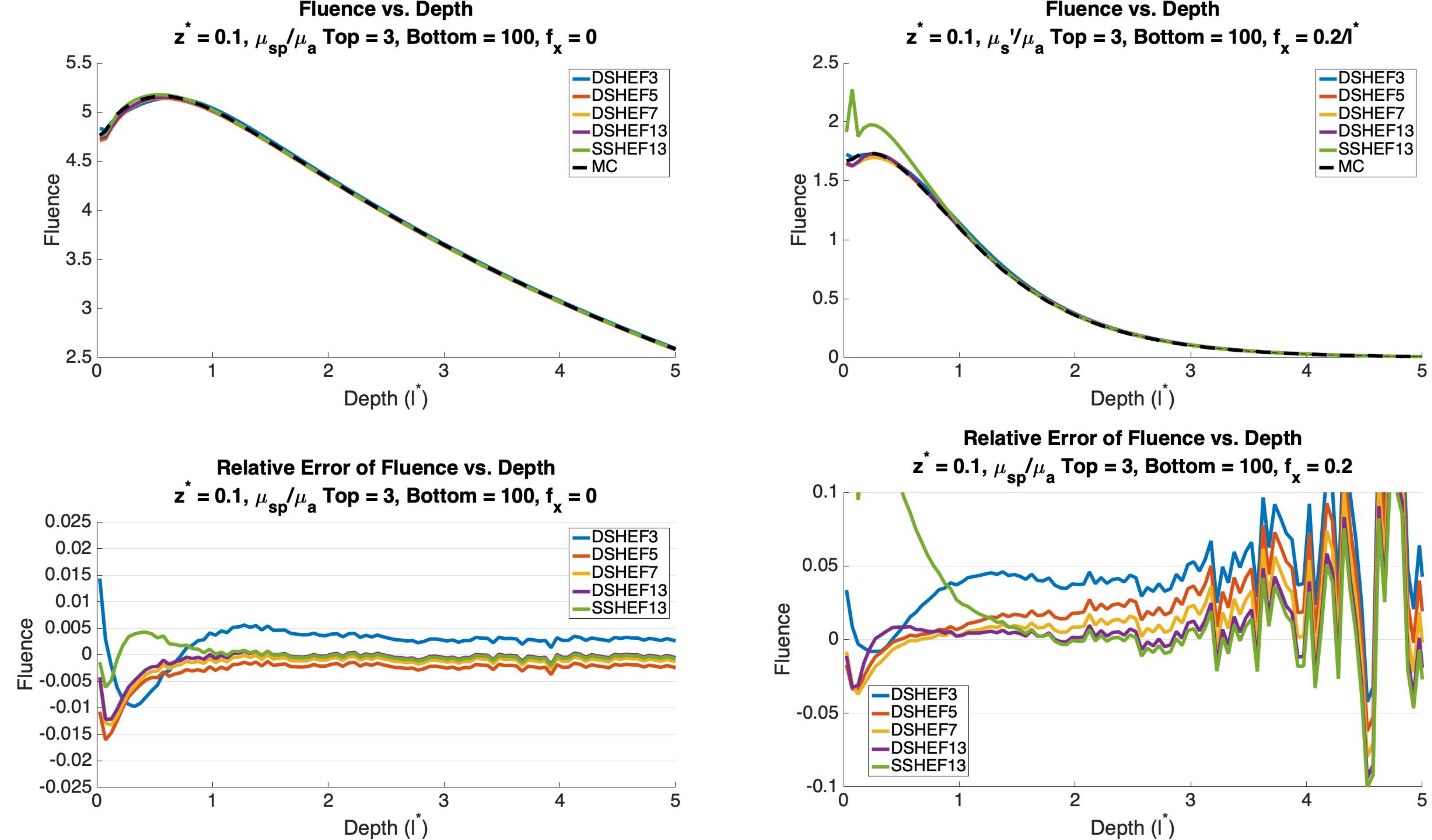

Fluence vs. Depth
z* = 0.1, μsp/μa Top = 3, Bottom = 100, fx = 0
Fluence
Depth (l*)
DSHEF3
DSHEF5
DSHEF7
DSHEF13
SSHEF13
MC
Fluence vs. Depth
z* = 0.1, μs'/μa Top = 3, Bottom = 100, fx = 0.2/l*
Fluence
Depth (l*)
DSHEF3
DSHEF5
DSHEF7
DSHEF13
SSHEF13
MC
Relative Error of Fluence vs. Depth
z* = 0.1, μsp/μa Top = 3, Bottom = 100, fx = 0
Fluence
Depth (l*)
DSHEF3
DSHEF5
DSHEF7
DSHEF13
SSHEF13
Relative Error of Fluence vs. Depth
z* = 0.1, μsp/μa Top = 3, Bottom = 100, fx = 0.2
Fluence
Depth (l*)
DSHEF3
DSHEF5
DSHEF7
DSHEF13
SSHEF13

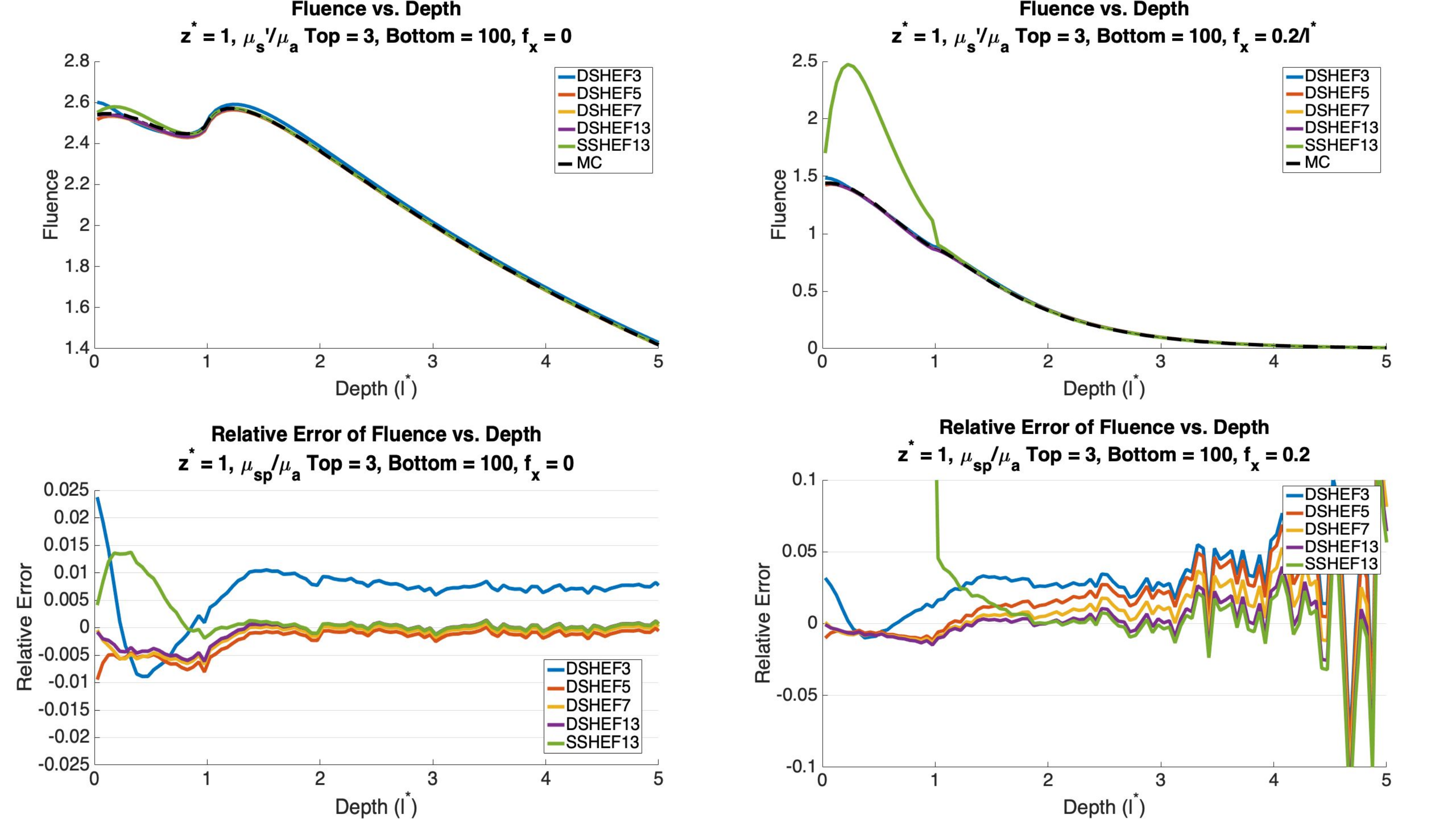

Fluence vs. Depth
$z^* = 1$, μ_s'/μ_a Top = 3, Bottom = 100, $f_x = 0$
Fluence
Depth (l^*)
DSHEF3
DSHEF5
DSHEF7
DSHEF13
SSHEF13
MC
Fluence vs. Depth
$z^* = 1$, μ_s'/μ_a Top = 3, Bottom = 100, $f_x = 0.2/l^*$
Fluence
Depth (l^*)
DSHEF3
DSHEF5
DSHEF7
DSHEF13
SSHEF13
MC
Relative Error of Fluence vs. Depth
$z^* = 1$, μ_{sp}/μ_a Top = 3, Bottom = 100, $f_x = 0$
Relative Error
Depth (l^*)
DSHEF3
DSHEF5
DSHEF7
DSHEF13
SSHEF13
Relative Error of Fluence vs. Depth
$z^* = 1$, μ_{sp}/μ_a Top = 3, Bottom = 100, $f_x = 0.2$
Relative Error
Depth (l^*)
DSHEF3
DSHEF5
DSHEF7
DSHEF13
SSHEF13

Computation Times

On "The Beast," with **2 Xenon X5650 @ 2.67 GHz** and **32 GB RAM**, the following computation times were observed by MATLab's "timeit()" function:

- $DSHEF_3$: 1.96s
- $DSHEF_5$: 3.25s
- $DSHEF_7$: 4.93s
- $DSHEF_{13}$: 14.39s
- $SSHEF_{13}$: 5.13s

A **10M photon packet discrete absorption weight monte carlo simulation** took **>24 hours** on the same machine.

Conclusions

1. Both **$SHEF_N$** and **$DSHEF_N$** are capable of **simulating radiance** in **layered media** using similar **boundary conditions**.
   a. These layers may be an **order of magnitude** thinner than l^*.
   b. Media need **not be scattering dominant**.

2. **$SHEF_N$** shows the **same difficulties** it did with with homogeneous media.
   a. **Not robust** to changes in **spatial frequency**, particularly when **$z > 0$**.
   b. Some of these **(reflectance)** are **exacerbated in layered media**.
   c. **$DSHEF_N$** shows the **same robustness** it did in **homogeneous media**.

Conclusion And Future Directions

We have seen:

1. A new **spectral RTE solution** based on **double spherical harmonics**
   a. **Robust** to changes in **spatial frequency** and **optical properties**
   b. Capable of reconstructing **angular discontinuities** at **medium boundaries**
   c. Encodes important **information about radiance** in **operator spectra**
2. A **boundary condition** for **$SHEF_N$** and **$DSHEF_N$** allowing them to simulate radiance in **layered media**
   a. Further evidence of **robustness** of **$DSHEF_N$**

Future Directions - Operator Spectra

We have seen that **radiance deep within a medium** can be predicted by **operator spectra**. A **more detailed understanding** of these **spectra** will enable:

1. The extraction of **other information** about **radiance** and **functionals thereof**.
2. An understanding of the **relation between desired accuracy**, **optical properties** and necessary **order of expansion**.
3. The **bypass** of **eigenvector decomposition**.
   a. Overwhelming **majority of computational expense** located in this step.

Future Directions - SFD Imaging/Spectrocopy

Spatial Frequency Domain Imaging and Spectroscopy (SFDI/S) measures the **reflectance of spatially modulated light** to infer physiological properties of tissue.

DSHEF$_N$, like **SHEF$_N$**, is well suited to this modality due to its use of a **single point source** in the Fourier Domain.

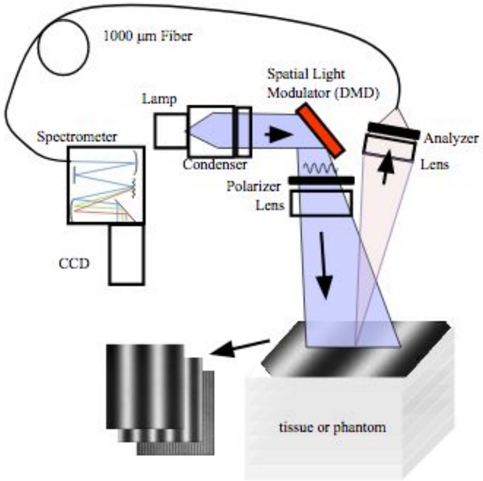

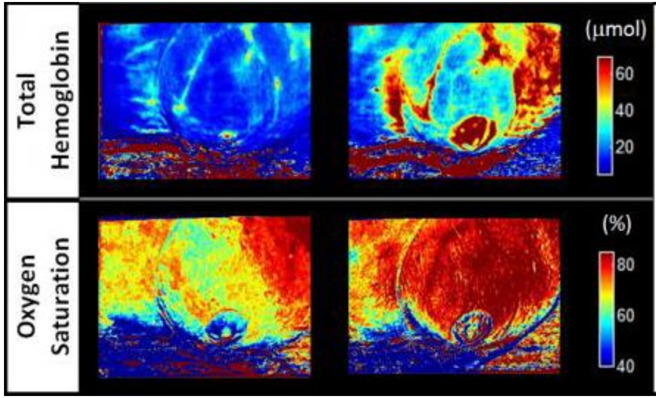

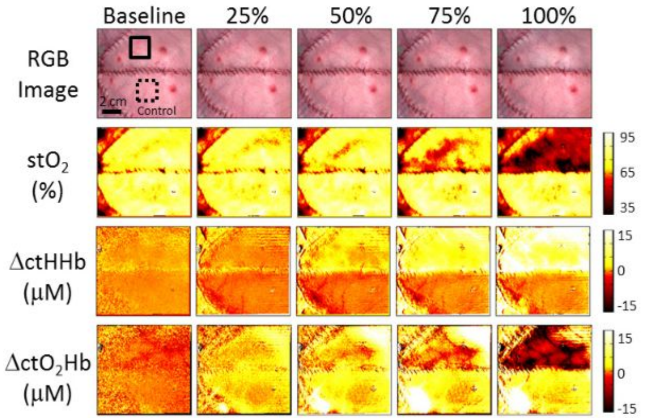

Image Credits, top left clockwise: Cuccia (2005), medgadget.com,

Future Directions - SFD Tomography

True depth resolved optical property recovery from SFD data remains **elusive**.

My ultimate goal with this research is to enable it using $DSHEF_N$ or a similar method. This will require **two major steps**:

1. Dropping assumption of layered, homogeneous tissue.
2. Efficient solution to the often ill-posed "backward problem."
   a. Machine learning
   b. Tikhonov regularization

References

[1] Steven L Jacques, "Optical properties of biological tissues: a review" 2013 *Phys. Med. Biol.* 58 R37

[2] Hui Fang *et al.*, "Noninvasive sizing of subcellular organelles with light scattering spectroscopy," in *IEEE Journal of Selected Topics in Quantum Electronics*, vol. 9, no. 2, pp. 267-276, March-April 2003, doi: 10.1109/JSTQE.2003.812515.

[3] Hayakawa CK, Spanier J, Venugopalan V. Comparative analysis of discrete and continuous absorption weighting estimators used in Monte Carlo simulations of radiative transport in turbid media. *J Opt Soc Am A Opt Image Sci Vis.* 2014;31(2):301-311. doi:10.1364/JOSAA.31.000301

[4] Akira Ishimaru, "Diffusion of light in turbid material," Appl. Opt. 28, 2210-2215 (1989)

[5] Kim A D and Keller J B, 'Light Propagation in Biological Tissue" 2003J. Opt. Soc. Am.A2092–8

[6] Manabu Machida *et al*, 'The Green's function for the radiative transport equation in the slab geometry" 2010 *J. Phys. A: Math. Theor.* 43 065402

References

[7] Stefan A. Carp, Scott A. Prahl, Vasan Venugopalan, "Radiative transport in the delta-P1 approximation: accuracy of fluence rate and optical penetration depth predictions in turbid semi-infinite media," J. Biomed. Opt. 9(3) (1 May 2004) https://doi.org/10.1117/1.1695412

[8] A. R. Gardner, A. D. Kim, and V. Venugopalan.Radiative transport produced by oblique illumination of turbid media with collimated beams.Physical Review E,87:063308, Jun 2013

[9] Gao H and Zhao HK,A fast forward solver of radiative transfer equation, Transport Theory and Statistical Physics38(2009), 149–192.

[10] Rolf B. Saager, David J. Cuccia, Anthony J. Durkin, "Determination of optical properties of turbid media spanning visible and near-infrared regimes via spatially modulated quantitative spectroscopy," J. Biomed. Opt. 15(1) 017012 (1 January 2010) https://doi.org/10.1117/1.3299322

[11] I. Seo, J. S. You, C. Hayakawa, and V. Venugopalan. Perturbation and differential MonteCarlo methods for measurement of optical properties in a layered epithelial tissue model.Journal of Biomedical Optics, 12:014030, 2007.

Acknowledgements

- Beckman Laser Institute
  - **Rolf Saager**
  - **Tony Durkin**
  - **Jerry Spanier**
  - Bruce Tromberg
  - Eric Potma
- Venugopalan Lab
  - **Vasan Venugopalan**
  - **Adam Gardner**
  - **Carole Hayakawa**
  - Janaka Ranasinghesagara
- Lowengrub Lab
  - **John Lowengrub**
- Math Department
  - Jun Allard
  - Jack Xin
  - Qing Nie
  - Dennis Eichorn
  - The Mathletes
- Center for Complex Biological Systems
  - **Karen Martin**
  - Arthur Lander
- UC Merced Applied Math
  - **Arnold Kim**
  - Chrysoula Tsogka
  - Camille Carvalho
- NSF IGERT
- NIH T32 EB009418
- NIBIB P41EB015890

Center for Complex Biological Systems
University of California, Irvine

Beckman Laser Institute & Medical Clinic
University of California · Irvine

Thank You!

Questions, comments, concerns, hate mail?